

Magnetic field dependence of critical currents of cross-type Josephson junctions with inhomogeneous critical current density under oblique magnetic fields

Soma Haraoka¹, Edmund Soji Otabe^{2,3}, and Yasunori Mawatari^{4*}

¹ *Department of Computer Science and Systems Engineering, Kyushu Institute of Technology, Fukuoka 820-8502, Japan.*

² *Department of Physics and Information Technology, Kyushu Institute of Technology, Fukuoka 820-8502, Japan.*

³ *Research Center for Neuromorphic AI Hardware, Kyushu Institute of Technology, Kitakyushu, Fukuoka 808-0135, Japan*

⁴ *National Institute of Advanced Industrial Science and Technology (AIST), Ibaraki 305-8568, Japan*

*E-mail: y.mawatari@aist.go.jp

Abstract

Studies of the magnetic interference of sandwich-type Josephson junctions in which perpendicular or oblique magnetic fields are applied to the junction plane have received less attention than those where the applied magnetic fields are parallel. Recently, it has been theoretically demonstrated that a variety of magnetic interferences of the critical currents appear when oblique magnetic fields are applied to a cross-type junction with homogeneous critical current density. We theoretically investigated the effect of the inhomogeneous critical current density in the junction plane, and found that more complicated magnetic interferences appeared. We considered the distribution of the current density flowing through the junction plane to explore the cause of these complex magnetic interferences.

1. Introduction

The magnetic field dependence of the DC critical currents in sandwich-type Josephson junctions shows a Fraunhofer-type interference pattern when a magnetic field is applied parallel to the junction plane.¹⁻⁴⁾ This magnetic interference is the basic principle for applications such as superconducting quantum interference devices.^{2, 4-6)} However, there are still only a few studies on magnetic interference in perpendicular or oblique magnetic fields. Rosenstein and Chen⁷⁾ as well as Hebard and Fulton⁸⁾ revealed that magnetic interference appears in overlap-type Josephson junctions under perpendicular magnetic fields. Miller *et al.*,⁹⁾ on the other hand, revealed that no magnetic interference appears in cross-type Josephson junctions under a perpendicular magnetic field. Monaco *et al.*^{10,11)} numerically and experimentally investigated the magnetic interference of various junction geometries under oblique magnetic fields. Furthermore, it was analytically demonstrated that anomalous magnetic interference patterns appear in cross-type junctions under oblique magnetic fields.¹²⁾

The magnetic interference of Josephson junctions is also affected by the distribution of the critical current density J_c in the junction area.^{4,13)} Analyses of magnetic interference of critical currents and inhomogeneity of J_c have been used to investigate the edge states in topological insulators.¹⁴⁻¹⁶⁾ In contrast to the work in Ref. 12, which focuses on cross-type junctions with homogeneous critical current density J_c , we also consider the effect of J_c inhomogeneity. We found that the magnetic interference patterns of cross-type junctions under oblique magnetic fields for inhomogeneous J_c show more complex and diverse patterns than for homogeneous J_c .

This paper consists of five sections including this section. The next section describes the theoretical model we used to consider the magnetic interference of cross-type Josephson junctions. The third section presents the results of the magnetic interference in oblique magnetic fields. In the fourth section, we consider the difference in magnetic interference for homogeneous and inhomogeneous J_c on the basis of the distribution of the current density flowing through the junction plane. The final section summarizes our results.

2. Theory

2.1 Cross-type junction

Figure 1 illustrates a cross-type Josephson junction consisting of two superconducting nanostrips and a barrier layer exposed to a magnetic field (H_x, H_y, H_z) . The top strip is

along the y axis, and the bottom strip is along the x axis. The two superconducting strips have the same width w and thickness d_s . The thickness of the barrier layer is d_j , and the junction area is a square measuring $w \times w$.

We assume that magnetic screening is weak in superconducting nanostrips (i.e., $d_s < \lambda_L$ and $w < \lambda_L^2/d_s$, where λ_L is the London penetration depth) and in small junctions (i.e., $w < \lambda_J^2/\lambda_L$, where λ_J is the Josephson length).¹⁷⁾ The effect of the self field due to the transport current is neglected.

2.2 Critical current

The current density flowing through the junction area $J_z(x, y)$ is given by

$$J_z(x, y) = J_c(x, y) \sin \theta(x, y), \quad (1)$$

where J_c is the critical current density. The gauge-invariant phase difference θ is expressed as $\theta(x, y) = \theta_0 + \theta_1(x, y)$, where θ_0 is a constant independent of the magnetic field and $\theta_1(x, y)$ for cross-type junctions is given by⁹⁾

$$\theta_1(x, y) = \frac{2x \pi \Phi_y}{w \phi_0} - \frac{2y \pi \Phi_x}{w \phi_0} - \frac{2xy \pi \Phi_z}{w^2 \phi_0}, \quad (2)$$

where $\Phi_x = \mu_0 H_x w d_{\text{eff}}$, $\Phi_y = \mu_0 H_y w d_{\text{eff}}$, and $\Phi_z = \mu_0 H_z w^2$ are the magnetic fluxes in the junction, ϕ_0 is the flux quantum, and d_{eff} is the effective barrier thickness given by $d_{\text{eff}} = d_j + d_s$.¹⁸⁾ The net current I_z flowing through the junction area is given by

$$\begin{aligned} I_z &= \int_{-w/2}^{w/2} dx \int_{-w/2}^{w/2} dy J_c(x, y) \sin \theta(x, y) \\ &= \int_{-w/2}^{w/2} dx \int_{-w/2}^{w/2} dy J_c(x, y) \sin[\theta_0 + \theta_1(x, y)] \\ &= \text{Im} [F \exp(i\theta_0)], \end{aligned} \quad (3)$$

where F is given by

$$F = \int_{-w/2}^{w/2} dx \int_{-w/2}^{w/2} dy J_c(x, y) \exp[i\theta_1(x, y)]. \quad (4)$$

The complex-valued function in Eq. (4) can be written as $F = |F| \exp(ig)$ with $g = \arg(F)$, and Eq. (3) yields

$$I_z = \text{Im}\{|F| \exp[i(\theta_0 + g)]\} = |F| \sin(\theta_0 + g). \quad (5)$$

Maximizing I_z with respect to θ_0 yields $I_z = |F|$ when $\theta_0 = \pi/2 - g = \pi/2 - \arg(F)$, and the critical current $I_c = |F|$ as a function of Φ_x , Φ_y , and Φ_z is thus given by

$$I_c(\Phi_x, \Phi_y, \Phi_z) = \left| \int_{-w/2}^{w/2} dx \int_{-w/2}^{w/2} dy J_c(x, y) \exp[i\theta_1(x, y)] \right|. \quad (6)$$

The critical current at zero magnetic field $I_{c0} = I_c(0,0,0)$ is given by

$$I_{c0} = \left| \int_{-w/2}^{w/2} dx \int_{-w/2}^{w/2} dy J_c(x, y) \right|. \quad (7)$$

For cross-type junctions with homogeneous J_c , analytical equations for Eq. (6) are available.¹²⁾ The current density in Eq. (1) when $I_z = I_c$ [i.e., $\theta_0 = \pi/2 - \arg(F)$] is

$$J_z(x, y) = J_c(x, y) \cos[\theta_1(x, y) - \arg(F)]. \quad (8)$$

3. Results

3.1 Inhomogeneous critical current density

As a model for inhomogeneous $J_c(x, y)$, we consider the case where J_c is piecewise constant. That is, $J_c = J_{c0}$ (where J_{c0} is constant) in the outer region of $x_0 < |x| < w/2$ or $y_0 < |y| < w/2$, whereas $J_c = 0$ in the inner region of $|x| < x_0$ and $|y| < y_0$ in the junction area. The magnetic interference is investigated for four cases of the parameters (x_0, y_0) shown in Fig. 2. For comparison, we also demonstrate the magnetic interference for the case of homogeneous J_c investigated in Ref. 12 [i.e., for $(x_0, y_0) = (0, 0)$ shown in Fig. 2(a)].

3.2 Critical currents under 2D oblique magnetic fields

Figure 3 depicts the critical currents of Eq. (6) as functions of Φ_x and Φ_z for $\Phi_y = 0$. The horizontal axis represents Φ_x/ϕ_0 , which is the normalized parallel magnetic field. The vertical axis represents Φ_z/ϕ_0 , which is the normalized perpendicular magnetic field. The color shade corresponds to the magnitude of I_c , where larger I_c is indicated by lighter colors.

Figure 4 depicts the I_c/I_{c0} as a function of Φ/ϕ_0 where $\Phi = \Phi_x$ or $\Phi = \Phi_z$. The blue line represents I_c/I_{c0} vs Φ_x/ϕ_0 for $\Phi_y = \Phi_z = 0$, while the orange line represents I_c/I_{c0} vs Φ_z/ϕ_0 for $\Phi_x = \Phi_y = 0$. Therefore, the blue line in Fig. 4 corresponds to I_c on the line $\Phi_z/\phi_0 = 0$ in Fig. 3, and similarly, the orange line in Fig. 4 corresponds to I_c on the line $\Phi_x/\phi_0 = 0$ in Fig. 3.

In the case of homogeneous J_c [Fig. 3(a)], we see no stripe pattern of $I_c(\Phi_x, 0, \Phi_z)$ when $|\Phi_z| > 2|\Phi_x|$, indicating that magnetic interference does not occur.¹²⁾ On the other hand, in the case of inhomogeneous J_c [Figs. 3(b)–(d)], magnetic interference occurs even

when $|\Phi_z| > 2|\Phi_x|$, and further unexpected magnetic interference is observed. Furthermore, in the case of $(x_0, y_0) = (0.4, 0.4)w$, a Fraunhofer-like interference appears under perpendicular magnetic fields as well [orange line in Fig. 4(b)], in contrast to the absence of the magnetic interference for homogeneous J_c [orange line in Fig. 4(a)]. This phenomenon constitutes a critical difference between homogeneous J_c and inhomogeneous J_c .

3.3 Critical currents under 3D oblique magnetic fields

Figure 5 depicts the critical currents as functions of Φ_x , Φ_y , and Φ_z . The horizontal axis represents Φ_x/ϕ_0 , and the vertical axis represents Φ_y/ϕ_0 . The color legend for Fig. 5 is the same as that for Fig. 3. Figure 5 shows the cases where Φ_z/ϕ_0 is an integer ($\Phi_z/\phi_0 = 0, 1, 5, \text{ and } 10$); we also examined the cases where Φ_z/ϕ_0 is a half-integer, but found no clear difference. We see that various magnetic interferences appear depending on the inhomogeneity of J_c . The I_c plot for $(x_0, y_0) = (0.2, 0.4)w$ (not shown in Fig. 5) is the same as Fig. 5(c) for $(x_0, y_0) = (0.4, 0.2)w$ with Φ_x and Φ_y interchanged.

4. Discussion

Figure 6 depicts the current density $J_z(x, y) = J_c(x, y) \sin[\theta(x, y)]$ across the junction plane when $I_z = I_c$ under a perpendicular magnetic field of $\Phi_z/\phi_0 = 4$, obtained from Eqs. (2), (4), and (8). In our piecewise constant J_c model, as in Sec. 3.1, we have $J_z(x, y)/J_{c0} = \cos[\theta_1(x, y) - \arg(F)]$ for $x_0 < |x| < w/2$ or $y_0 < |y| < w/2$, whereas $J_z(x, y) = 0$ for $|x| < x_0$ and $|y| < y_0$. Figure 6(a) shows J_z for homogeneous J_c [$(x_0, y_0) = (0, 0)$], and Fig. 6(b) shows J_z for inhomogeneous J_c [$(x_0, y_0) = (0.4, 0.4)w$].

As shown in Fig. 6(a), J_z is strongly modulated near the four corners of the junction plane, but less modulated near the center of the junction plane. Consequently, the positive and negative J_z do not cancel out, resulting in no magnetic interference under perpendicular magnetic fields for homogeneous J_c . On the other hand, as shown in Fig. 6(b), J_z is modulated over the entire region of the junction plane where $J_c = J_{c0} > 0$, and positive and negative J_z tend to cancel out, resulting in magnetic interference.

Contrary to our model, if J_c is distributed only near the center of the junction plane, the magnetic interference is equivalent to the case where the junction plane size is small with homogeneous J_c . Therefore, in this case, magnetic interference does not appear under perpendicular magnetic fields.

In an overlap-type junction, as shown in Fig. 7, superconducting strips are arranged parallel to each other along the longitudinal direction (as opposed to the transverse arrangement in cross-type junctions), overlapping extremities of the strips.^{4,7,8,10,11} Further details on the distinction between cross-type and overlap-type junctions, particularly regarding the magnetic interference in perpendicular magnetic fields, can be found in Refs. 10 and 11. Although we also considered the impact of inhomogeneous J_c in overlap-type junctions (not included in the present paper), our examination revealed that variations in J_c do not yield significant difference in the magnetic interference of overlap-type junctions.

5. Conclusion

We theoretically investigated the magnetic interferences of DC critical currents of cross-type junctions with inhomogeneous critical current density J_c under oblique magnetic fields. We found that variations in the J_c distribution generate a variety of complex magnetic interferences under oblique magnetic fields. When the J_c near the edges was larger than that near the center of the junction plane, a clear magnetic interference appeared even under perpendicular magnetic fields. The mechanism of the magnetic interference was discussed. It is important that the current density near the center of the junction plane is hardly modulated under perpendicular magnetic field.

Acknowledgment

This study has been supported by JSPS KAKENHI, Grant No. JP20K05314.

References

- 1) J. M. Rowell, Phys. Rev. Lett. **11**, 200 (1963).
- 2) R. C. Jaklevic, J. Lambe, A. H. Silver, and J. E. Mercereau, Phys. Rev. Lett. **12**, 159 (1964).
- 3) B. D. Josephson, Adv. Phys. **14**, 419 (1965).
- 4) A. Barone and G. Paterno, Physics and Applications of the Josephson Effect (New York: Wiley, 1982).
- 5) J. Clarke, Proc. IEEE, **77**, 1208 (1989).
- 6) J. Clarke and A. I. Braginski (eds), The SQUID Handbook (New York: Wiley, 2004).
- 7) I. Rosenstein and J. T. Chen, Phys. Rev. Lett. **35**, 303 (1975).
- 8) A. F. Hebard and T. A. Fulton, Phys. Rev. Lett. **35**, 1310 (1975).

- 9) S. L. Miller, K. R. Biagi, J. R. Clem, and D. K. Finnemore, *Phys. Rev. B* **31**, 2684 (1985).
- 10) R. Monaco, M. Aaroe, J. Mygind, and V. P. Koshelets, *J. Appl. Phys.* **104**, 023906 (2008).
- 11) R. Monaco, M. Aaroe, J. Mygind, and V. P. Koshelets, *Phys. Rev. B* **79**, 144521 (2009).
- 12) Y. Mawatari, *J. Phys. D* **55**, 200002 (2022).
- 13) R. C. Dynes and T. A. Fulton, *Phys. Rev. B* **3**, 3015 (1971).
- 14) J. H. Lee, G.-H. Lee, J. Park, J. Lee, S.-G. Nam, Y.-S. Shin, J. S. Kim, and H.-J. Lee, *Nano Lett.* **14**, 5029 (2014).
- 15) S. Hart, H. Ren, T. Wagner, P. Leubner, M. Mühlbauer, C. Brüne, H. Buhmann, L. W. Molenkamp, and A. Yacoby, *Nat. Phys.* **10**, 638 (2014).
- 16) V. S. Pribiag, A. J. A. Beukman, F. Qu, M. C. Cassidy, C. Charpentier, W. Wegscheider, and L. P. Kouwenhoven, *Nat. Nanotechnol.* **10**, 593 (2015).
- 17) J. R. Clem, *Phys. Rev. B* **81**, 144515 (2010).
- 18) M. Weihnacht, *Phys. Status Solidi b*, **32**, K169 (1969).

Figure Captions

Fig. 1. Schematic of a cross-type junction with a barrier layer at $|x| \leq w/2$, $|y| \leq w/2$, and $|z| < d_j/2$. The top superconducting strip is located at $|x| < w/2$, $|y| < \infty$, and $d_j/2 < z < d_j/2 + d_s$. The bottom strip is located at $|x| < \infty$, $|y| < w/2$, and $-d_j/2 - d_s < z < -d_j/2$.

Fig. 2. Models of the J_c distribution in the junction plane: $J_c = J_{c0}$ (where J_{c0} is a constant) for $x_0 < |x| < w/2$ or $y_0 < |y| < w/2$, whereas $J_c = 0$ for $|x| < x_0$ and $|y| < y_0$ in the junction area. (a) Homogeneous J_c with $(x_0, y_0) = (0, 0)$, (b) inhomogeneous J_c with $(x_0, y_0) = (0.4, 0.4)w$, (c) $(x_0, y_0) = (0.4, 0.2)w$, and (d) $(x_0, y_0) = (0.2, 0.4)w$.

Fig. 3. Contour plots of the critical currents $I_c(\Phi_x, 0, \Phi_z)/I_{c0}$ under 2D magnetic fields for (a) $(x_0, y_0) = (0, 0)w$, (b) $(x_0, y_0) = (0.4, 0.4)w$, (c) $(x_0, y_0) = (0.4, 0.2)w$, and (d) $(x_0, y_0) = (0.2, 0.4)w$. The horizontal axis Φ_x/ϕ_0 is the normalized parallel magnetic field, and the vertical axis Φ_z/ϕ_0 is the normalized perpendicular magnetic field.

Fig. 4. DC critical currents under a 1D magnetic field Φ/ϕ_0 where $\Phi = \Phi_x$ or $\Phi = \Phi_z$ for (a) $(x_0, y_0) = (0, 0)$, and (b) $(x_0, y_0) = (0.4, 0.4)w$, where the blue line represents $I_c(\Phi_x, 0, 0)/I_{c0}$, and the orange line represents $I_c(0, 0, \Phi_z)/I_{c0}$.

Fig. 5. Contour plots of the critical currents $I_c(\Phi_x, \Phi_y, \Phi_z)/I_{c0}$ under 3D magnetic fields for (a) $(x_0, y_0) = (0, 0)w$ (top panels), (b) $(x_0, y_0) = (0.4, 0.4)w$ (middle panels), and (c) $(x_0, y_0) = (0.4, 0.2)w$ (bottom panels). The horizontal axis is Φ_x/ϕ_0 , and the vertical axis is Φ_y/ϕ_0 .

Fig. 6. Current density $J_z(x, y)$ across the junction plane for $I_z = I_c$ under a perpendicular field of $\Phi_z/\phi_0 = 4$ for (a) $(x_0, y_0) = (0, 0)w$ and (b) $(x_0, y_0) = (0.4, 0.4)w$.

Fig. 7. Schematic of an overlap-type junction with a barrier layer sandwiched by two superconducting strips.

Figures

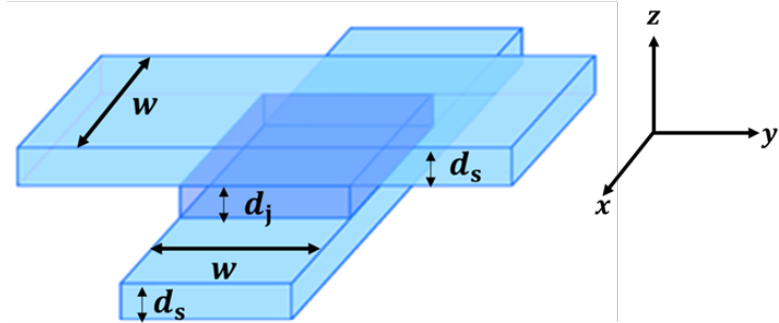


Fig. 1

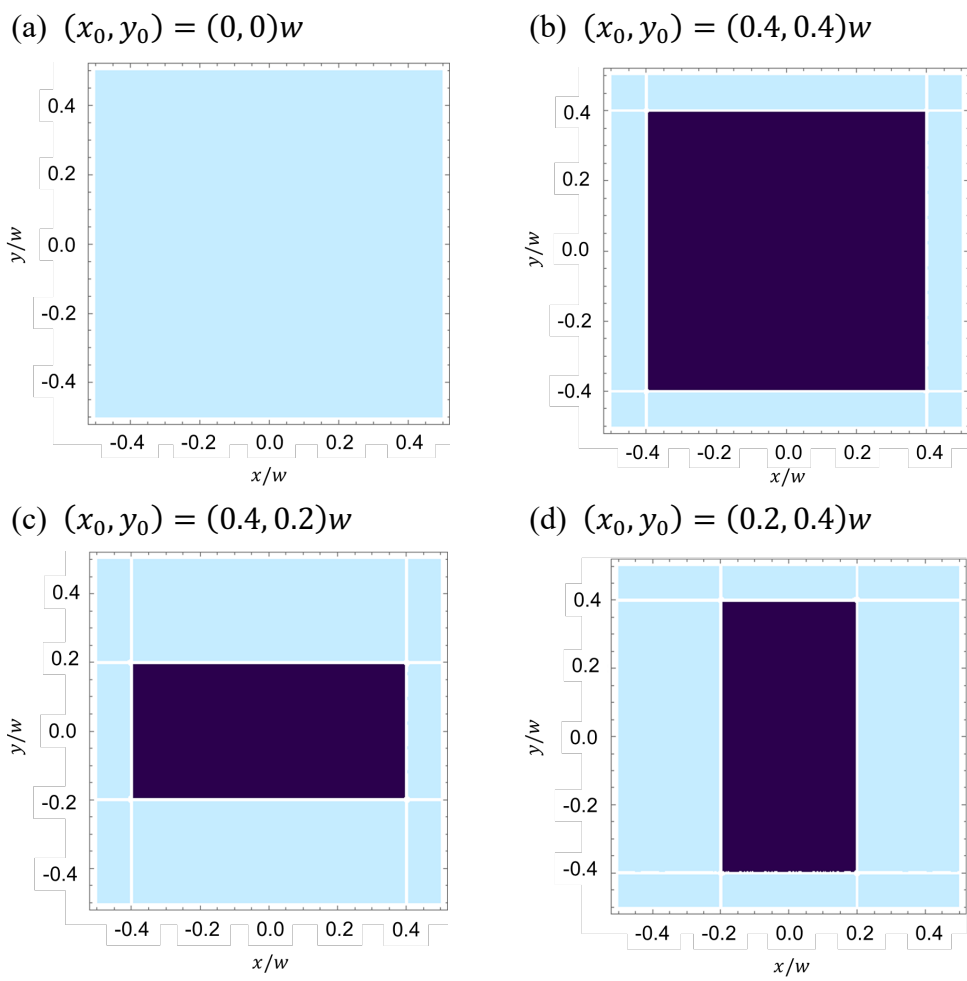
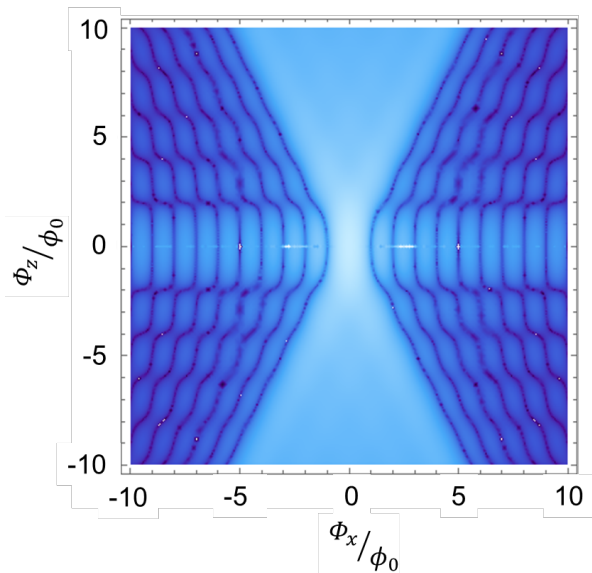
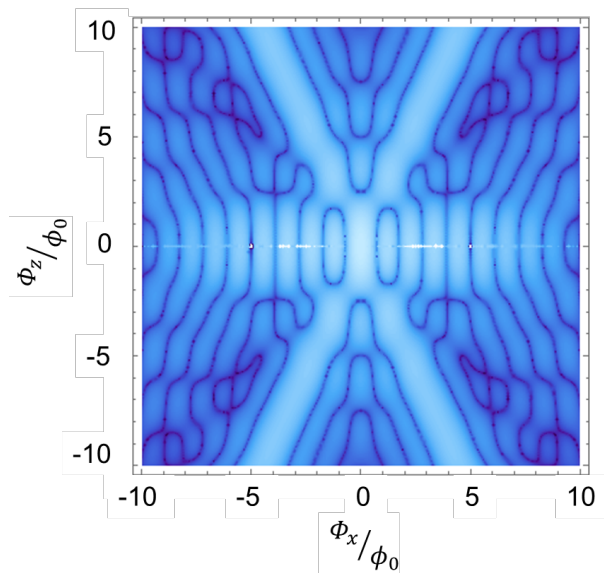


Fig. 2

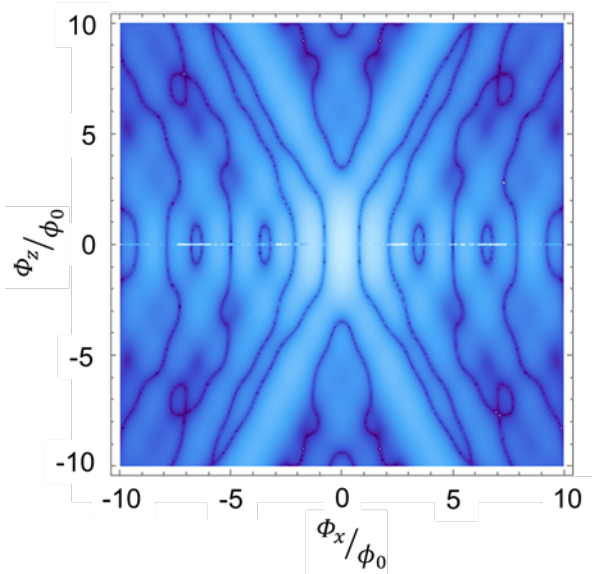
(a) $(x_0, y_0) = (0, 0)w$



(b) $(x_0, y_0) = (0.4, 0.4)w$



(c) $(x_0, y_0) = (0.4, 0.2)w$



(d) $(x_0, y_0) = (0.2, 0.4)w$

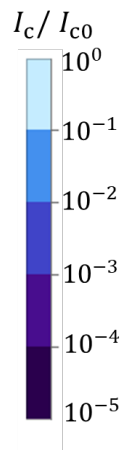
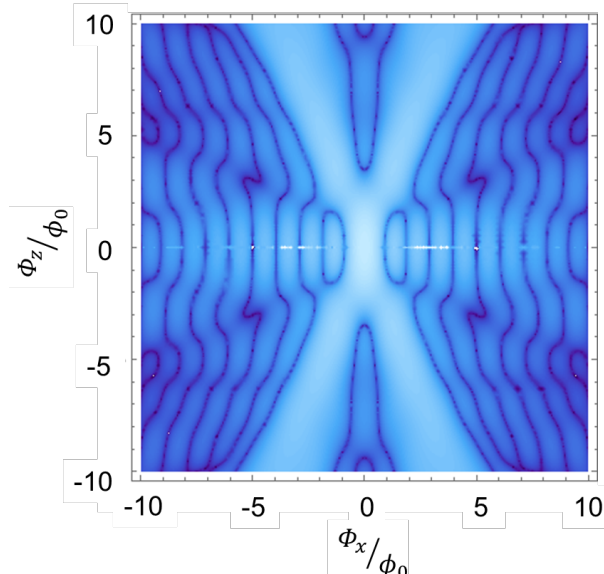


Fig. 3

(a) $(x_0, y_0) = (0, 0)w$

(b) $(x_0, y_0) = (0.4, 0.4)w$

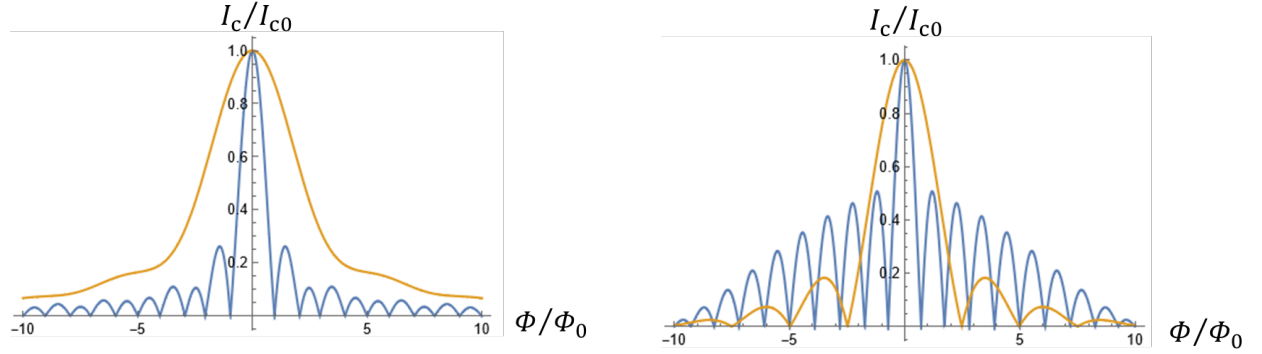


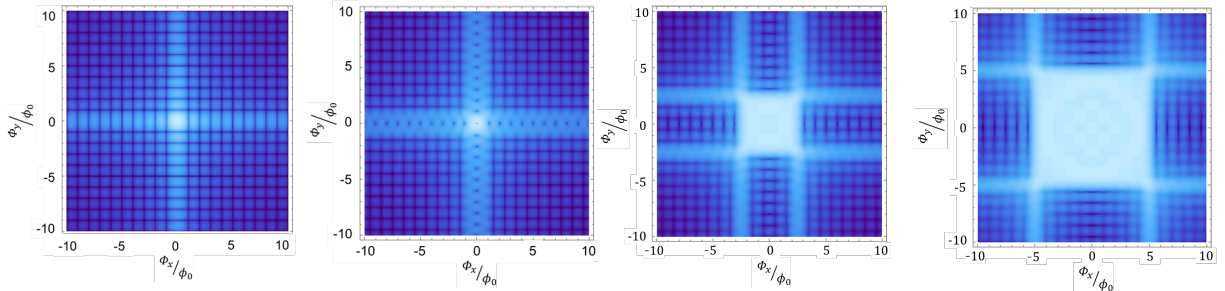
Fig. 4

(a-1) $\Phi_z/\phi_0 = 0$

(a-2) $\Phi_z/\phi_0 = 1$

(a-3) $\Phi_z/\phi_0 = 5$

(a-4) $\Phi_z/\phi_0 = 10$

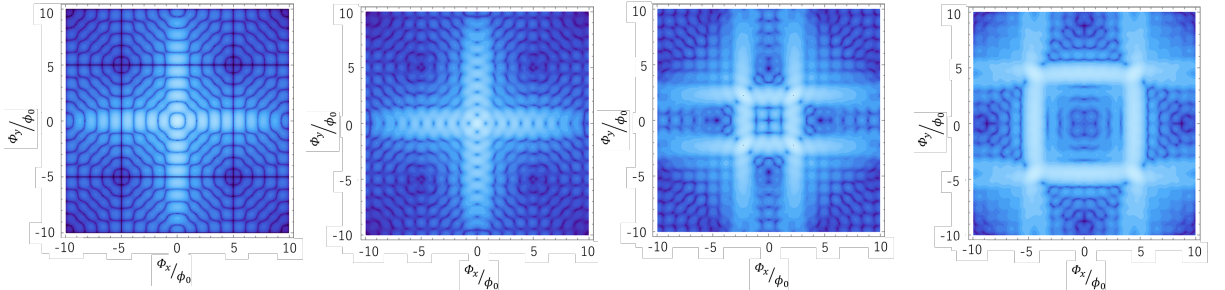


(b-1) $\Phi_z/\phi_0 = 0$

(b-2) $\Phi_z/\phi_0 = 1$

(b-3) $\Phi_z/\phi_0 = 5$

(b-4) $\Phi_z/\phi_0 = 10$



(c-1) $\Phi_z/\phi_0 = 0$

(c-2) $\Phi_z/\phi_0 = 1$

(c-3) $\Phi_z/\phi_0 = 5$

(c-4) $\Phi_z/\phi_0 = 10$

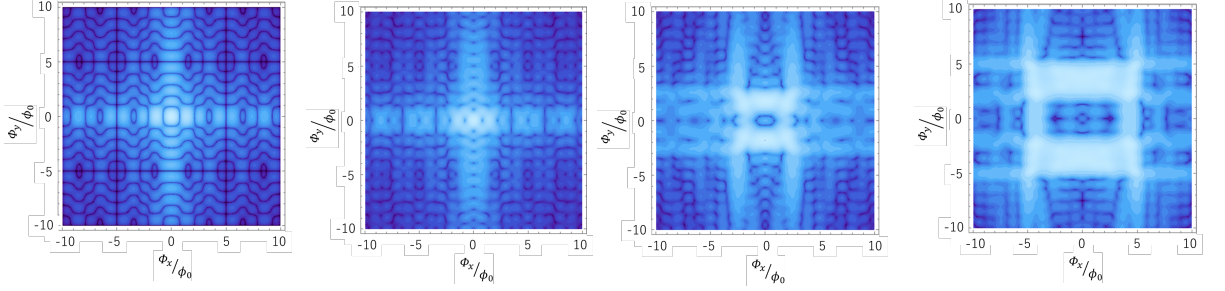
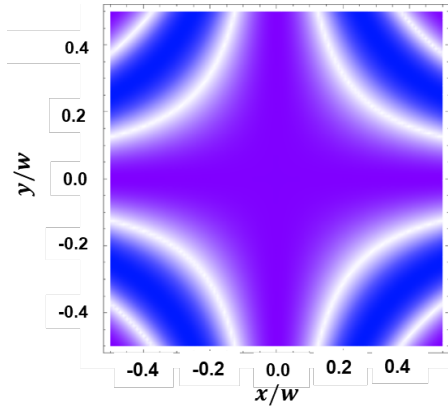
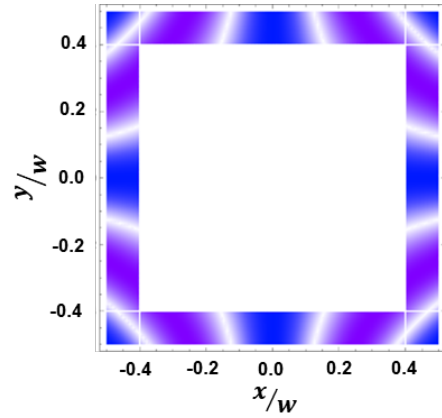


Fig. 5

(a) $(x_0, y_0) = (0, 0)w$



(b) $(x_0, y_0) = (0.4, 0.4)w$



J_z/J_{c0}

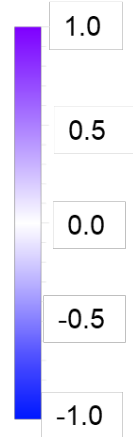


Fig. 6

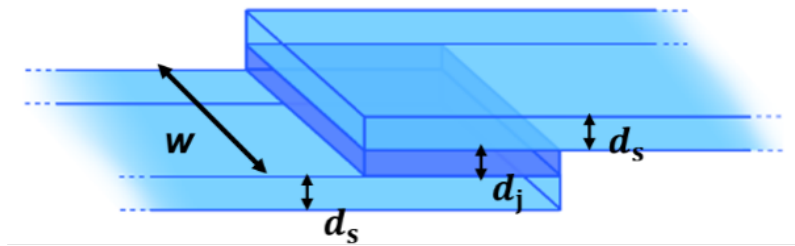


Fig. 7